Selective Recognition of a DNA G-Quadruplex by an Engineered Antibody[†]

Himesh Fernando, Raphaël Rodriguez, and Shankar Balasubramanian*

The University Chemical Laboratory, University of Cambridge, Lensfield Road, Cambridge, CB2 1EW, U.K.

Received May 23, 2008; Revised Manuscript Received July 10, 2008

ABSTRACT: Particular guanine rich nucleic acid sequences can fold into stable secondary structures called G-quadruplexes. These structures have been identified in various regions of the genome that include the telomeres, gene promoters and UTR regions, raising the possibility that they may be associated with biological function(s). Computational analysis has predicted that intramolecular G-quadruplex forming sequences are prevalent in the human genome, thus raising the desire to differentially recognize genomic G-quadruplexes. We have employed antibody phage display and competitive selection techniques to generate a single-chain antibody that shows >1000-fold discrimination between G-quadruplex and duplex DNA, and furthermore >100-fold discrimination between two related intramolecular parallel DNA G-quadruplexes. The amino acid sequence composition at the antigen binding site shows conservation within the light and heavy chains of the selected scFvs, suggesting sequence requirements for G-quadruplex recognition. Circular dichroism (CD) spectroscopic data showed that the scFv binds to the prefolded G-quadruplex and does not induce G-quadruplex structure formation. This study demonstrates the strongest discrimination that we are aware of between two intramolecular genomic G-quadruplexes.

G-rich nucleic acid sequences have the potential to fold into four stranded structures called G-quadruplexes (*1*). Such structures comprise tetragonal arrays of mutually hydrogen-bonded guanines called G-tetrads that stack to form a G-quadruplex helix. There are various classes of G-quadruplex structure that can form, depending on strand molecularity, and within each class, there are subtypes that vary according to the strand polarities. In particular, intramolecular G-quadruplexes can form from sequences that contain four sets of tandem Gs, each separated by intervening sequences that may form the loops of the G-quadruplex. While there are studies that predict the folded conformation of intramolecular G-quadruplexes on the basis of the lengths of the loops (*2, 3*), it has been shown that intramolecular G-quadruplexes have a general tendency to be conformationally polymorphic (*4, 5*). The sequence and structure of G-quadruplex loops present the potential for a given G-quadruplex to be distinct at the molecular level.

Intramolecular G-quadruplex-forming motifs are prevalent in the human genome. Computational studies have predicted approximately 370,000 putative G-quadruplex-forming sequences throughout the human genome (*6, 7*), among which approximately 226,000 are unique in sequence (*7*). This has raised the challenge of elucidating whether G-quadruplexes are associated with biological function. There are now a number of hypotheses linking G-quadruplex motifs with function that include the association between telomeric G-quadruplexes and telomere maintenance (*8*), and the association between G-quadruplexes in the promoters of protein coding genes and transcription (*9*). There are also numerous natural G-quadruplex-binding proteins that have been identified (*10*−*12*), further suggesting a biological function of G-quadruplexes.

It has been a major goal to address the selective molecular recognition of intramolecular DNA G-quadruplexes. While the G-tetrads of G-quadruplexes are the core structural feature, the loops and grooves may provide the molecular basis for selective recognition. G-quadruplex-binding small molecules that interact primarily via the external G-tetrads have been designed (*13*), of which some have shown good discrimination between G-quadruplex and duplex DNA (*14*−*16*). Recently, there have been some examples of small molecules that show some discrimination (up to 10-fold) between G-quadruplexes (*17*−*20*). Another strategy has been to select or engineer proteins that recognize particular G-quadruplexes. Indeed, zinc finger proteins have been engineered that recognize intramolecular G-quadruplex structures with very high selectivity as compared to duplex DNA (*21, 22*). Antibodies have been generated that recognize the *Stylonychia* intermolecular G-quadruplex, of which one was found to strongly discriminate a parallel G-quadruplex from an antiparallel G-quadruplex (*23*).

Herein we report on a single-chain variable fragment (scFv[1]) antibody selected by phage display and competitive selection that binds to a human parallel intramolecular DNA G-quadruplex with high affinity. The antibody strongly discriminates between two parallel intramolecular G-quadruplexes, each found in the promoter of the *c-kit* proto-oncogene.

[†] This research was supported by a programme grant from Cancer Research UK. H.F. was funded by Cambridge Commonwealth Trusts.

* To whom correspondence should be addressed. Tel: (+) 44 1223 336 347. Fax: (+) 44 1223 336 913. E-mail: sb10031@cam.ac.uk.

[1] Abbreviations: UTR, untranslated region; CD, circular dichroism; scFv, single-chain variable fragment; CDR, complementarity determining region; CDRH, complementarity determining region heavy chain; CDRL, complementarity determining region light chain; ssDNA, single strand DNA; SPR, surface plasmon resonance; SLE, systemic lupus erythematosus.

10.1021/bi800983u CCC: $40.75
Published on Web 08/15/2008

Table 1: Biopanning Details for the Selection of c-kit2 G-Quadruplex Binding scFvs

			Pan 3				Pan 4			
	pan 1	pan 2	test[a]	control 1[b]	control 2[c]	control 3[d]	test1[a]	test 2[a]	control 1[c]	control 2[d]
coating G-quadruplex c-kit2 (nM)	2000	2000	1000	1000	1000	none	20	500	20	none
applied phage conc. (phage per mL)	10^{13}	10^{13}	10^{13}	10^{13}	10^{13}	10^{13}	10^{13}	10^{13}	10^{13}	10^{13}
no. of washes	10	20	20	20	20	20	20	20	20	20
competitor	none	none	1 μM duplex DNA 1 μM random ssDNA library	1 μM duplex DNA	none	none	1 μM c-kit1 G-quadruplex	1 μM c-kit1 G-quadruplex	none	none
eluate phage conc. (phage per mL)	4×10^6	2×10^9	8×10^6	8×10^6	2×10^7	2×10^4	7×10^7	2×10^8	3×10^7	1×10^6

[a] Panning used for the amplification and selection of c-kit2 binding scFvs. [b] To determine depletion of the library by random ssDNA. [c] To determine depletion of the library by all competitor DNA. [d] To determine background phage titer.

MATERIALS AND METHODS

Sample Preparation. The DNA oligonucleotide samples d(biotin-[$AG_3AG_3CGCTG_3AG_2AG_3$]) (c-kit1), d(biotin-[$CG_3CG_3CGCGAG_3AG_4$]) (c-kit2), d(biotin-[G_3CGCG_3-AGGAATTG$_3$CG$_3$]) (bcl2Mid), d(biotin-[$TGAG_3$-$TG_3TAG_3TG_3TAA$]) (MYC22-G14T/G23T), d(biotin-[GGCATAGTGCGTGGGCGTTAGC]) and its nonbiotinylated complementary strand (duplex DNA), were purchased from Sigma Genosys. Ten micromolar stock solutions were prepared in 50 mM Tris-HCl (pH 7.4) containing 100 mM KCl. The samples were heated to 90 °C for 10 min and annealed over a period of 14 h at a rate of 0.1 °C/min down to 4 °C and maintained at 4 °C overnight. For the salt deficient CD experiments, samples were prepared by dissolving the DNA in 50 mM Tris-HCl (pH 7.4) without temperature controlled annealing.

Biopanning. Phage produced from the Tomlinson J library were used to pan against the biotinylated c-kit2 G-quadruplex coated onto a streptavidin immunotube. The panning protocol used was essentially as described in the MRC protocol (http://www.geneservice.co.uk/products/proteomic/datasheets/tomlinsonIJ.pdf), but Tris-HCl containing 100 mM KCl instead of PBS was used to maintain the G-quadruplex conformation. Briefly, the streptavidin immunotubes were coated with 2 mL of biotinylated G-quadruplex DNA solution overnight, followed by blocking and a washing step. 10^{13} phages were applied to bind, unbound phages were washed away, and the bound phages were eluted using trypsin. *E. coli* TG1 were infected with the eluted phage for amplification. Where competitor DNA was used, the phages were allowed to equilibrate with the competitor DNA for 1 h at room temperature before being allowed to bind to the c-kit2 G-quadruplex on the immunotube. Details of each pan are given in Table 1. Immunotubes were coated with two concentrations of c-kit2 G-quadruplex in the final pan, 20 nM (test 1) and 500 nM (test 2).

Expression of scFvs and ELISA. Expression of soluble scFvs and ELISA were conducted as mentioned in the MRC protocol (http://www.geneservice.co.uk/products/proteomic/datasheets/tomlinsonIJ.pdf). Briefly, individual colonies of HB2151 infected with the eluted phage were grown in 96 well microtiter plates till $OD_{600\ nm}$ was approximately 0.9 and then were induced with IPTG. Soluble scFvs were expressed at 30 °C overnight and transferred onto another microtiter plate coated with the target DNA G-quadruplex to carry out single well ELISA. The standard ELISA protocol was followed, but 50 mM Tris-HCl containing 100 mM KCl instead of PBS was used to maintain the G-quadruplex conformation. Protein A-HRP was used to detect the scFvs bound to the G-quadruplex. Approximately 400 colonies (~200 from test 1 and ~200 from test 2) from the final pan eluate were screened by single well ELISA for c-kit2 G-quadruplex binding. The wells that produced the highest signal intensity in the single well ELISA were selected for further analysis. This included a total of 8 clones from tests 1 and 2.

Phagemid DNA Sequencing. pIT2 phagemid vectors containing the insert for scFv were sequenced using LMB3 (5′-CAG GAA ACA GCT ATG AC-3′) sequencing primer.

Surface Plasmon Resonance. Surface plasmon resonance measurements were performed on a BIAcore 3000 biosensor system (Biacore Inc.) using a streptavidin-coated sensor chip (SA). Biotinylated c-kit1, biotinylated c-kit2, and biotinylated duplex DNA were annealed in running buffer containing 50 mM Tris-HCl (pH 7.4), 100 mM KCl, and immobilized (450 RU) in flow cells. DNA binding experiments were carried out by using the same running buffer but containing calf thymus DNA (15 μg/ml), at a flow rate of 20 μL min^{-1} by using the KINJECT command for 4 min followed by a dissociation phase of 3 min. The sensor chip was regenerated by injecting a 1 M KCl solution for 1 min followed by running buffer for 1 min. Dissociation constants were determined with the global fitting method by using the binding model with mass transfer (Biaevaluation 3.0.2).

CD Spectroscopy. Circular dichroism spectra were obtained on a Jasco J-810 spectropolarimeter. The wavelength was varied from 220 to 320 nm at a rate of 50 nm/min. Measurements were made at 20 °C using a quartz cell with a path length of 1 cm. Each spectrum reported is an average of 5 scans. The samples were prepared to a final oligonucleotide concentration of 1 μM in 50 mM Tris-HCl (pH 7.4) and 100 mM KCl. For each experiment, a CD spectrum of the buffer was recorded and subtracted from the spectrum obtained for the DNA-containing solution.

RESULTS AND DISCUSSION

We previously identified two intramolecular G-quadruplex-forming sequences in the promoter of the proto-oncogene *c-kit* (c-kit1 and c-kit2) (Figure 1A) (*24, 25*). The *c-kit* gene encodes a receptor tyrosine kinase that has importance in

A

c-kit1:	d(A**GGGAGGGCGCTGGGAGGAGGG**)
c-kit2:	d(C**GGGCGGGCGCGAGGGAGGGG**)
bcl2Mid:	d(**GGGCGCGGGAGGAATTGGGCGGG**)
MYC22-G14T/G23T:	d(TGA**GGGTGGGTAGGGTGGGTAA**)
Duplex DNA:	5'-d(GGCATAGTGCGTGGGCGTTAGC)-3'
	3'-d(CCGTATCACGCACCCGCAATCG)-5'

B

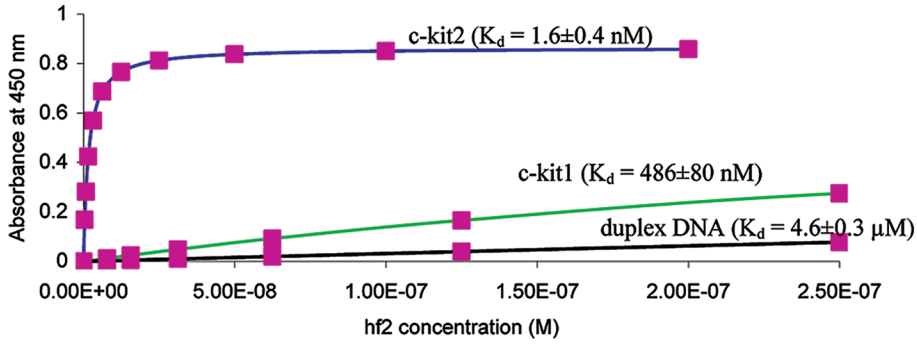

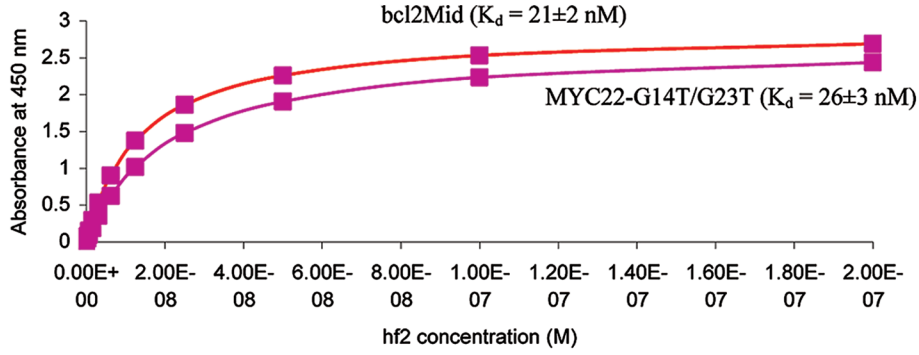

C

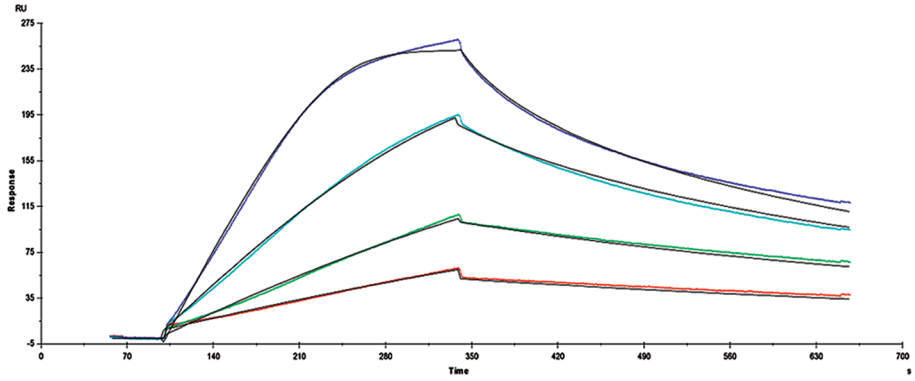

FIGURE 1: (A) Target DNA sequences and their binding interactions with hf2 scFv. DNA sequences of c-kit1, c-kit2, bcl2Mid, MYC22-G14T/G23T, and duplex DNA. Guanines involved in the formation of a G-tetrad are shown in bold. (B) ELISA binding curves of hf2-DNA interactions. (Top) hf2 binding c-kit2 G-quadruplex, K_d of 1.6 ± 0.4 nM (blue); c-kit1 G-quadruplex, K_d of 486 ± 80 nM (green); and duplex DNA, K_d of 4.6 ± 0.3 μM (black). (Bottom) hf2 binding bcl2Mid G-quadruplex, K_d of 21 ± 2 nM (red) and MYC22-G14T/G23T G-quadruplex, K_d of 26 ± 3 nM (cerise). (C) Sensorgram overlays of hf2 scFv at 6.1 nM (red), 12.2 nM (green), 25 nM (cyan), and 50 nM (blue) concentrations interacting with the c-kit2 G-quadruplex. The black lines indicate the Biaevaluation 3.0 global fitting of the binding kinetics.

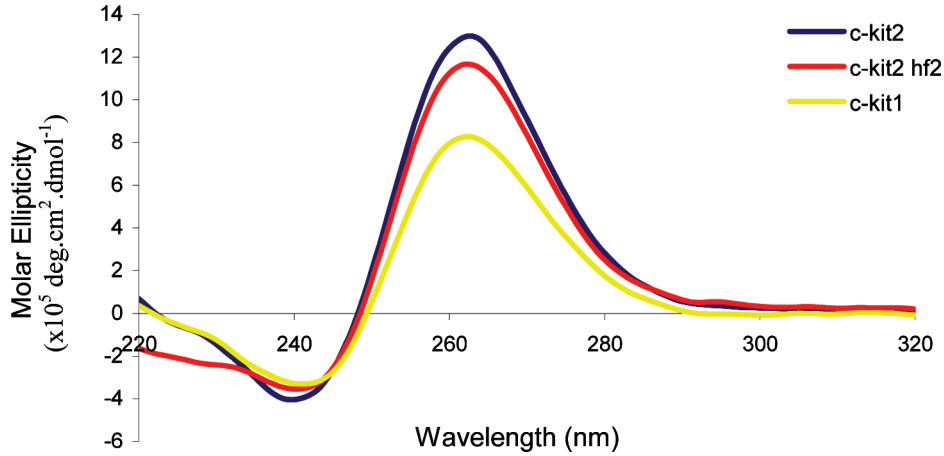

FIGURE 2: CD spectra of 1 μM c-kit1 (yellow), 1 μM c-kit2 (blue), and 1 μM c-kit2 with 1 μM hf2 (red) in 50 mM Tris-HCl containing 100 mM KCl.

Table 2: Sequences of scFvs That Bind to the c-kit2 G-Quadruplex[a]

Clone	K_d(nM) c-kit2	K_d(nM) c-kit1	Ratio K_d (c-kit1/c-kit2)	CDRH2	CDRH3	CDRL2	CDRL3
				52a	96 98	50 53	91 96
hf2	1.6	480	300	TIPRHGQGTSYADSVKG	NATLFDY	RASHLQS	QQSPRRPPT
hf3	21	483	23	KIDRSGTTTRYADSVKG	TSRRFDY	RASVLQS	QQVRRRPST
hf4	16	225	14	QINRMGNSTTYADSVKG	AGRRFDY	RASKLQS	QQRIARPAT
hf5	45	636	14	TIAGRGRTTQYADSVKG	GLRSFDY	RASRLQS	QQSGMGPRT
hf6	30	284	9	TITRSGAKTFYADSVKG	SSRRFDY	RASRLQS	QQGRQQPPT
hf7	22	136	6	GIASRGVQTAYADSVKG	NRNLFDY	RASHLQS	QQGKHRPPT
hf8	45	197	4	SINPVGQKTTYADSVKG	GYKIFDY	RASILQS	QQGAQPPFT
Hf9	185	341	2	SISRTGLPTRYADSVKG	GNYRFDY	NASGLQS	QQARRRPTT

[a] The CDR regions are numbered as defined by Kabat (*48*). Amino acid positions within VH and VL (CDRH and CDRL columns). The randomised residues are underlined. Residues within conserved regions are boxed.

cell signaling and the control of cell proliferation. Elevated levels of *c-kit* expression have been reported in most gastrointestinal cancers (*26*), hence making it a prime anticancer target. The G-quadruplex-forming sequences c-kit1 and c-kit2 are located between −89 and −160 bp upstream of the transcription start site, and the two sequences are separated by 29 bp. The G-quadruplex structure formed by c-kit1 has been solved by high resolution ^{1}H NMR spectroscopy and shown to form a parallel G-quadruplex of unusual structure in which a G that appears to be in a loop region is in fact part of a G-tetrad (Figure 1) (*27*). ^{1}H NMR and circular dichroism spectroscopic studies on c-kit2 have suggested that the majority of the population folds into a parallel conformation (Figure 2) (*24*). We set out to explore whether the folded parallel topologies of c-kit1 and c-kit2 could be differentially recognized by an antibody.

The antibody was selected using phage display (*28*) of the Tomlinson J library (*29*) that comprises ~1.4 × 10^8 human scFv variants. The antibody library has been constructed (*29*) by randomizing a total of 18 positions in the complementarity determining regions (CDR) 2 and 3 of heavy and light chains (NNK encodes all amino acids including the TAG stop codon). The randomized amino acid positions are H50, H52, H52a, H53, H55, H56, H58, H95, H96, H97, and H98 of CDR heavy chain (CDRH), and L50, L53, L91, L92, L93, L94, and L96 of CDR light chain (CDRL). Recent publications report that the library has produced scFvs that bind to a variety of targets including bovine complex I (*30*), Microcystin LR (*31*), SARS coronovirus (*32*), and fibrin (*33*). We are not aware of any reports of its use in nucleic acid recognition. The phage-displayed antibodies were selected using immobilized c-kit2 intramolecular DNA G-quadruplex in the presence of competitor DNA in the mobile phase to impose negative selection. The competitor regime comprised varying levels of guanine-rich double strand DNA (duplex DNA), a library of random single strand DNA (ssDNA), and the folded c-kit1 intramolecular G-quadruplex (see the Materials and Methods section for details). We screened the eluate of the fourth and final pan for scFvs that bind to c-kit2 by ELISA assay. Of these, we then evaluated eight clones for discrimination between c-kit1 and c-kit2 G-quadruplexes (Table 2).

hf2 Binds to the c-kit2 G-Quadruplex with High Selectivity. Using an ELISA binding assay (*21*), hf2 was found to bind the DNA G-quadruplex formed by the c-kit2 sequence with a K_d of 1.6 ± 0.4 nM, whereas the K_d of hf2 for G-rich 22

bp duplex DNA was 4.6 ± 0.3 μM (Figure 1B), indicating that hf2 had approximately 3000-fold lower affinity for the duplex than for c-kit2. The ELISA-based K_d of hf2 for the G-quadruplex formed by the c-kit1 sequence was 486 ± 80 nM. Thus, hf2 had ~300-fold weaker affinity for the c-kit1 intramolecular G-quadruplex as compared to the c-kit2 G-quadruplex (Figure 1B). It is the highest discrimination that has been reported between two intramolecular genomic DNA G-quadruplexes. We confirmed the interaction between hf2 and the various DNA targets by using surface plasmon resonance (SPR) experiments using the global fitting method (*22*) (Figure 1C). Its k_{on} was 6.84×10^6 M^{-1} s^{-1}, and k_{off} was 0.0566 s^{-1}. Thus, the measured K_d for this interaction using kinetics is 8 nM, a slightly higher value than that obtained by ELISA. We were unable to detect specific binding of hf2 to c-kit1 or duplex DNA at concentrations up to 400 nM. The SPR measurements were consistent with the high specificity of hf2 observed by ELISA.

The c-kit2 sequence is unique in the human genome, suggestive of the potential for distinct structural features that could be exploited for molecular recognition. As yet, a structure for the c-kit2 G-quadruplex has not been solved. However, on the basis of 1-D NMR and CD spectroscopic studies c-kit2 appears to form a mixture of parallel and antiparallel structures, where the parallel structure is the dominant G-quadruplex form (*24*). The c-kit1 sequence is also unique in the human genome, and NMR spectroscopic studies have suggested a single folded conformation. The NMR structure of c-kit1 (*27*) confirms an overall parallel conformation with a distinct folding topology (*34*). While the G-tetrad cores of the c-kit1 and c-kit2 G-quadruplexes share similar features, it is the topology and sequence of the loops that are likely to provide the distinguishing features of c-kit2 and of c-kit1 for differential molecular recognition by hf2.

c-kit2 Binding scFvs Have Conserved Amino Acids. To further understand the nature of scFv and c-kit G-quadruplex interaction, we analyzed the amino acid sequences of hf2 and seven other scFvs (hf3-hf9) that recognize c-kit2 G-quadruplex. The seven other scFvs had ELISA K_d values ranging from 21 nM to 185 nM for c-kit2 and ELISA K_d values ranging from 136 nM to 636 nM for c-kit1. Thus, their ability to discriminate between c-kit1 and c-kit2 ranged from 2-fold to 23-fold (Table 2).

Alignment of the primary amino acid sequences of hf2-hf9 made it evident that certain randomized positions in both CDRH and CDRL favored particular amino acids (Table 2). Position L50 of CDRL2 had arginine in 7 out of 8 clones. Position L53 (CDRL2) also showed strong bias for basic residues in 5 of the clones. Amino acid conservation in the CDRL3 is less pronounced but shows an enrichment of arginine in the region between L91 and L94 and some preference for proline at position L96. Within the heavy chain (CDRH), the majority of the scFvs had arginine at position H52a of CDR2 and basic residues at positions between H96 and H98 of CDR3. Previous reports of double strand DNA binding antibodies isolated from phage display libraries or patients with systemic lupus erythematosus (SLE) autoimmune disease, when compared with normal antibody population, showed an enrichment of arginine, asparagine, and lysine amino acids in their CDRs that can participate in charge interactions or hydrogen bond with DNA phosphates or bases (*35*−*37*). While the G-quadruplex binding antibodies we analyzed did not show a general enrichment of asparagines and lysine, they do show an enrichment of arginine in CDRs of both heavy and light chains. The CDRH3 is considered the most important hypervariable loop for antigen−antibody interactions (*38*). Several other studies found clustering of arginine residues, particularly in the CDRH3 for double strand DNA-binding antibodies isolated from SLE patients or mouse models (*37, 39, 40*). Similarly, most of the clones analyzed for c-kit2 G-quadruplex binding also showed clustering of arginine in the CDRH3 suggesting a similarity in the type of interaction between the residues of CDRH3 and the two types of DNA structures. It is noteworthy that the clone hf2, which discriminated best between the two G-quadruplexes, is an exception to this conservation since it completely lacks basic amino acids in its CDRH3.

hf2 Prefers c-kit2 G-Quadruplex over Randomly Selected G-Quadruplexes. We were interested to determine whether hf2 could discriminate between the c-kit2 G-quadruplex, for which it was selected, and various randomly chosen human intramolecular G-quadruplexes, which were not employed in the negative selection regime. To address this, we chose two examples of well-characterized G-quadruplexes. One was bcl2Mid (also called bcl2MidG4Pu23-G15T/G16T), a mixed-type G-quadruplex (*41*), and MYC22-G14T/G23T, a parallel G-quadruplex (*42*) (Figure 1A). The solution structures of both G-quadruplexes have been solved by high resolution NMR spectroscopy. ELISA binding studies showed that hf2 bound bcl2Mid with a K_d of 21 ± 2 nM and to MYC22-G14T/G23T with a K_d of 26 ± 3 nM, affinities approximately 15-fold weaker than the hf2−c-kit2 interaction (Figure 1B). Although the discrimination for bcl2Mid and MYC22-G14T/G23T over c-kit2 is not as large as that observed between c-kit1 and c-kit2, hf2 clearly maintains the strongest affinity to its intended target over randomly selected G-quadruplexes. This supports that achieving specificity for a particular intramolecular G-quadruplex by a protein is feasible. The observation also suggests that the nature of the sequences employed in the negative selection regime is important for the profile of selectivity.

c-kit2 G-Quadruplex Conformation Is Unaffected on hf2 Binding. To address whether hf2 affected c-kit2 structure upon binding, we carried out a circular dichroism (CD) spectroscopic study. CD spectroscopy can provide valuable insights into the folding and strand orientation of G-quadruplexes. Parallel and antiparallel strand orientations give characteristic CD spectra (*43*−*46*). The CD spectrum of c-kit2 shows a predominant parallel signature with a positive CD signal at 263 nm and a negative signal at 240 nm (Figure 2). Figure 2 shows the CD spectra of c-kit2 (1 μM) obtained in Tris-HCl buffer containing 100 mM KCl in the presence and absence of the hf2 antibody (1 μM) under conditions where the DNA is fully complexed by the antibody (K_d of 1.6 ± 0.4 nM). The data show that hf2 does not alter the form of the c-kit2 CD spectrum, which supports that the hf2−c-kit2 complex still comprises a parallel folded G-quadruplex. When the experiment was repeated, but without the presence of stabilizing KCl (*47*), the inclusion of hf2 did not induce further formation of G-quadruplex as judged by the CD spectrum (Supporting Information). This

suggests that hf2 recognizes and binds to a prefolded G-quadruplex and that it does not promote G-quadruplex formation.

CONCLUSIONS

To the best of our knowledge, the single chain antibody hf2 is the first reported example of a molecule that shows large discrimination (>100-fold) between 2-folded intramolecular DNA G-quadruplexes formed from human genomic sequences. While G-quadruplexes share structural features and commonly exhibit structural polymorphism, it has been suggested that the loops offer the potential for discrimination at the molecular level. We hypothesize that loop recognition forms the basis of discriminating c-kit2 from c-kit1 by hf2. This proof-of-concept suggests that specificity of G-quadruplex recognition is certainly achievable. Highly specific antibodies that recognize a particular G-quadruplex sequence and structure provide a potential means to demonstrate the existence of such structures in cells. An example of this is the use of an antibody to reveal the existence of G-quadruplex DNA in the telomeres of *Stylonychia* (*23*). We now intend to explore whether the antibodies we have described in this article are sufficiently selective to detect the presence of a quadruplex in the promoter of *c-kit*.

ACKNOWLEDGMENT

We thank MRC Geneservice for providing us with the Tomlinson IJ Library. We thank Dr. Sylvain Ladame of Institut de Science et Ingénierie Supramoléculaires, Université Louis Pasteur-CNRS, 8 allée Gaspard Monge, 67083 Strasbourg, France for his assistance with surface plasmon resonance data analysis. We are grateful to Dr. Sven Sewitz of the Department of Chemistry, University of Cambridge for careful proofreading of the manuscript.

SUPPORTING INFORMATION AVAILABLE

One figure that shows CD spectra of c-kit2 (1 μM) obtained in 50 mM Tris-HCl buffer in the presence and absence of hf2 antibody (1 μM). This material is available free of charge via the Internet at http://pubs.acs.org.

REFERENCES

1. Henderson, E., Hardin, C. C., Walk, S. K., Tinoco, I., Jr., and Blackburn, E. H. (1987) Telomeric DNA oligonucleotides form novel intramolecular structures containing guanine-guanine base pairs. *Cell 51*, 899–908.
2. Hazel, P., Huppert, J., Balasubramanian, S., and Neidle, S. (2004) Loop-length-dependent folding of G-quadruplexes. *J. Am. Chem. Soc. 126*, 16405–16415.
3. Bugaut, A., and Balasubramanian, S. (2008) A sequence-independent study of the influence of short loop lengths on the stability and topology of intramolecular DNA G-quadruplexes. *Biochemistry 47*, 689–697.
4. Seenisamy, J., Rezler, E. M., Powell, T. J., Tye, D., Gokhale, V., Joshi, C. S., Siddiqui-Jain, A., and Hurley, L. H. (2004) The dynamic character of the G-quadruplex element in the c-MYC promoter and modification by TMPyP4. *J. Am. Chem. Soc. 126*, 8702–8709.
5. Dai, J., Carver, M., and Yang, D. (2008) Polymorphism of human telomeric quadruplex structures. *Biochimie 90*, 1172−1183.
6. Huppert, J. L., and Balasubramanian, S. (2005) Prevalence of quadruplexes in the human genome. *Nucleic Acids Res. 33*, 2908–2916.
7. Todd, A. K., Johnston, M., and Neidle, S. (2005) Highly prevalent putative quadruplex sequence motifs in human DNA. *Nucleic Acids Res. 33*, 2901–2907.
8. Zahler, A. M., Williamson, J. R., Cech, T. R., and Prescott, D. M. (1991) Inhibition of telomerase by G-quartet DNA structures. *Nature 350*, 718–720.
9. Siddiqui-Jain, A., Grand, C. L., Bearss, D. J., and Hurley, L. H. (2002) Direct evidence for a G-quadruplex in a promoter region and its targeting with a small molecule to repress c-MYC transcription. *Proc. Natl. Acad. Sci. U.S.A. 99*, 11593–11598.
10. Giraldo, R., and Rhodes, D. (1994) The yeast telomere-binding protein RAP1 binds to and promotes the formation of DNA quadruplexes in telomeric DNA. *EMBO J. 13*, 2411–2420.
11. Paeschke, K., Simonsson, T., Postberg, J., Rhodes, D., and Lipps, H. J. (2005) Telomere end-binding proteins control the formation of G-quadruplex DNA structures in vivo. *Nat. Struct. Mol. Biol. 12*, 847–854.
12. Fry, M. (2007) Tetraplex DNA and its interacting proteins. *Front. Biosci. 12*, 4336–4351.
13. Clark, G. R., Pytel, P. D., Squire, C. J., and Neidle, S. (2003) Structure of the first parallel DNA quadruplex-drug complex. *J. Am. Chem. Soc. 125*, 4066–4067.
14. Kim, M. Y., Vankayalapati, H., Shin-Ya, K., Wierzba, K., and Hurley, L. H. (2002) Telomestatin, a potent telomerase inhibitor that interacts quite specifically with the human telomeric intramolecular g-quadruplex. *J. Am. Chem. Soc. 124*, 2098–2099.
15. Monchaud, D., and Teulade-Fichou, M. P. (2008) A hitchhiker's guide to G-quadruplex ligands. *Org. Biomol. Chem. 6*, 627–636.
16. Schouten, J. A., Ladame, S., Mason, S. J., Cooper, M. A., and Balasubramanian, S. (2003) G-quadruplex-specific peptide-hemicyanine ligands by partial combinatorial selection. *J. Am. Chem. Soc. 125*, 5594–5595.
17. Waller, Z. A., Shirude, P. S., Rodriguez, R., and Balasubramanian, S. (2008) Triarylpyridines: a versatile small molecule scaffold for G-quadruplex recognition. *Chem. Commun. (Cambridge)* 1467–1469.
18. Bejugam, M., Sewitz, S., Shirude, P. S., Rodriguez, R., Shahid, R., and Balasubramanian, S. (2007) Trisubstituted isoalloxazines as a new class of G-quadruplex binding ligands: small molecule regulation of c-kit oncogene expression. *J. Am. Chem. Soc. 129*, 12926–12927.
19. Bugaut, A., Jantos, K., Wietor, J. L., Rodriguez, R., Sanders, J. K., and Balasubramanian, S. (2008) Exploring the differential recognition of DNA G-quadruplex targets by small molecules using dynamic combinatorial chemistry. *Angew. Chem., Int. Ed. 47*, 2677–2680.
20. Jantos, K., Rodriguez, R., Ladame, S., Shirude, P. S., and Balasubramanian, S. (2006) Oxazole-based peptide macrocycles: a new class of G-quadruplex binding ligands. *J. Am. Chem. Soc. 128*, 13662–13663.
21. Isalan, M., Patel, S. D., Balasubramanian, S., and Choo, Y. (2001) Selection of zinc fingers that bind single-stranded telomeric DNA in the G-quadruplex conformation. *Biochemistry 40*, 830–836.
22. Ladame, S., Schouten, J. A., Roldan, J., Redman, J. E., Neidle, S., and Balasubramanian, S. (2006) Exploring the recognition of quadruplex DNA by an engineered Cys2-His2 zinc finger protein. *Biochemistry 45*, 1393–1399.
23. Schaffitzel, C., Berger, I., Postberg, J., Hanes, J., Lipps, H. J., and Plückthun, A. (2001) In vitro generated antibodies specific for telomeric guanine-quadruplex DNA react with Stylonychia lemnae macronuclei. *Proc. Natl. Acad. Sci. U.S.A. 98*, 8572–8577.
24. Fernando, H., Reszka, A. P., Huppert, J., Ladame, S., Rankin, S., Venkitaraman, A. R., Neidle, S., and Balasubramanian, S. (2006) A conserved quadruplex motif located in a transcription activation site of the human c-kit oncogene. *Biochemistry 45*, 7854–7860.
25. Rankin, S., Reszka, A. P., Huppert, J., Zloh, M., Parkinson, G. N., Todd, A. K., Ladame, S., Balasubramanian, S., and Neidle, S. (2005) Putative DNA quadruplex formation within the human c-kit oncogene. *J. Am. Chem. Soc. 127*, 10584–10589.
26. Sakurai, S., Fukasawa, T., Chong, J. M., Tanaka, A., and Fukayama, M. (1999) C-kit gene abnormalities in gastrointestinal stromal tumors (tumors of interstitial cells of Cajal). *Jpn. J. Cancer Res. 90*, 1321–1328.
27. Phan, A. T., Kuryavyi, V., Burge, S., Neidle, S., and Patel, D. J. (2007) Structure of an unprecedented G-quadruplex scaffold in the human c-kit promoter. *J. Am. Chem. Soc. 129*, 4386–4392.
28. Smith, G. P. (1985) Filamentous fusion phage: novel expression vectors that display cloned antigens on the virion surface. *Science 228*, 1315–1317.

29. de Wildt, R. M., Mundy, C. R., Gorick, B. D., and Tomlinson, I. M. (2000) Antibody arrays for high-throughput screening of antibody-antigen interactions. *Nat. Biotechnol. 18*, 989–994.
30. Rubinstein, J. L., Holt, L. J., Walker, J. E., and Tomlinson, I. M. (2003) Use of phage display and high-density screening for the isolation of an antibody against the 51-kDa subunit of complex I. *Anal. Biochem. 314*, 294–300.
31. McElhiney, J., Lawton, L. A., and Porter, A. J. (2000) Detection and quantification of microcystins (cyanobacterial hepatotoxins) with recombinant antibody fragments isolated from a naive human phage display library. *FEMS Microbiol. Lett. 193*, 83–88.
32. Liu, Z. X., Yi, G. H., Qi, Y. P., Liu, Y. L., Yan, J. P., Qian, J., Du, E. Q., and Ling, W. F. (2005) Identification of single-chain antibody fragments specific against SARS-associated coronavirus from phage-displayed antibody library. *Biochem. Biophys. Res. Commun. 329*, 437–444.
33. Yan, J. P., Ko, J. H., and Qi, Y. P. (2004) Generation and characterization of a novel single-chain antibody fragment specific against human fibrin clots from phage display antibody library. *Thromb. Res. 114*, 205–211.
34. Todd, A. K., Haider, S. M., Parkinson, G. N., and Neidle, S. (2007) Sequence occurrence and structural uniqueness of a G-quadruplex in the human c-kit promoter. *Nucleic Acids Res. 35*, 5799–5808.
35. Stollar, B. D. (1994) Molecular analysis of anti-DNA antibodies. *FASEB J. 8*, 337–342.
36. Barry, M. M., Mol, C. D., Anderson, W. F., and Lee, J. S. (1994) Sequencing and modeling of anti-DNA immunoglobulin Fv domains. Comparison with crystal structures. *J. Biol. Chem. 269*, 3623–3632.
37. Barbas, S. M., Ditzel, H. J., Salonen, E. M., Yang, W. P., Silverman, G. J., and Burton, D. R. (1995) Human autoantibody recognition of DNA. *Proc. Natl. Acad. Sci. U.S.A. 92*, 2529–2533.
38. Kuby, J. (1997) *Immunology*, 3rd ed., W. H. Freeman and Company.
39. Krishnan, M. R., Jou, N. T., and Marion, T. N. (1996) Correlation between the amino acid position of arginine in VH-CDR3 and specificity for native DNA among autoimmune antibodies. *J. Immunol. 157*, 2430–2439.
40. Guth, A. M., Zhang, X., Smith, D., Detanico, T., and Wysocki, L. J. (2003) Chromatin specificity of anti-double-stranded DNA antibodies and a role for Arg residues in the third complementarity-determining region of the heavy chain. *J. Immunol. 171*, 6260–6266.
41. Dai, J., Dexheimer, T. S., Chen, D., Carver, M., Ambrus, A., Jones, R. A., and Yang, D. (2006) An intramolecular G-quadruplex structure with mixed parallel/antiparallel G-strands formed in the human BCL-2 promoter region in solution. *J. Am. Chem. Soc. 128*, 1096–1098.
42. Ambrus, A., Chen, D., Dai, J., Jones, R. A., and Yang, D. (2005) Solution structure of the biologically relevant G-quadruplex element in the human c-MYC promoter. Implications for G-quadruplex stabilization. *Biochemistry 44*, 2048–2058.
43. Ambrus, A., Chen, D., Dai, J., Bialis, T., Jones, R. A., and Yang, D. (2006) Human telomeric sequence forms a hybrid-type intramolecular G-quadruplex structure with mixed parallel/antiparallel strands in potassium solution. *Nucleic Acids Res. 34*, 2723–2735.
44. Wang, Y., and Patel, D. J. (1993) Solution structure of the human telomeric repeat d[AG3(T2AG3)3] G-tetraplex. *Structure 1*, 263–282.
45. Jin, R., Gaffney, B. L., Wang, C., Jones, R. A., and Breslauer, K. J. (1992) Thermodynamics and structure of a DNA tetraplex: a spectroscopic and calorimetric study of the tetramolecular complexes of d(TG3T) and d(TG3T2G3T). *Proc. Natl. Acad. Sci. U.S.A. 89*, 8832–8836.
46. Parkinson, G. N., Lee, M. P., and Neidle, S. (2002) Crystal structure of parallel quadruplexes from human telomeric DNA. *Nature 417*, 876–880.
47. Mergny, J. L., Phan, A. T., and Lacroix, L. (1998) Following G-quartet formation by UV-spectroscopy. *FEBS Lett. 435*, 74–78.
48. Kabat, E. A., Wu, T. T., Perry, H. M., Gottesman, K. S., and Foeller, C. (1991) *Sequences of Proteins of Immunological Interest*, 5th ed., U.S. Department of Health and Human Services, Washington DC.

BI800983U